Word count 6912 (excluding references)

A ligand-specific kinetic switch regulates glucocorticoid receptor trafficking and function.

Peter J Trebble[1,2], James M Woolven[3], Ken A Saunders[3], Karen D Simpson[3], Stuart N Farrow[1,3], Laura C Matthews[1,2]*, David W Ray[1,2]*

Running title: Ligand-specific regulation of GR action

[1] Manchester Centre for Nuclear Hormone Research in Disease, [2] Centre for Diabetes and Endocrinology, Institute for Human Development, Faculty of Medical and Human Sciences, University of Manchester, and Manchester Academic Health Sciences Centre, Manchester Royal Infirmary, Manchester, M13 9PT, United Kingdom. [3] Respiratory Therapy Area GlaxoSmithKline, Stevenage, SG1 2NY, United Kingdom.

*Address for correspondence,
AV Hill Building, University of Manchester, Manchester M139PT, UK
Phone 0161-275-5655
Fax 0161-275-5958
Email david.w.ray@manchester.ac.uk
Email laura.matthews@manchester.ac.uk

Key words:
Nuclear receptor; glucocorticoids; Heat shock protein 90; crystal structure; subcellular trafficking

JCS Advance Online Article. Posted on 17 May 2013

Abstract

The ubiquitously expressed glucocorticoid receptor (GR) is a major drug target for inflammatory disease, but issues of specificity, and target tissue sensitivity remain. We now identify high potency, non-steroidal GR ligands, GSK47867A and GSK47869A, which induce a novel conformation of the GR ligand binding domain (LBD) and augment the efficacy of cellular action. Despite their high potency GSK47867A and GSK47869A both induce surprisingly slow GR nuclear translocation, followed by prolonged nuclear GR retention, and transcriptional activity following washout. We reveal that GSK47867A and GSK47869A specifically alter the GR LBD structure at the HSP90 binding site. The alteration in HSP90 binding site was accompanied by resistance to HSP90 antagonism, with persisting transactivation seen after geldanamycin treatment. Taken together, our studies reveal a novel mechanism governing GR intracellular trafficking regulated by ligand binding, which relies on a specific surface charge patch within the LBD. This conformational change permits extended GR action, likely due to altered GR-HSP90 interaction. This chemical series may offer anti-inflammatory drugs with prolonged duration of action due to altered pharmacodynamics rather than altered pharmacokinetics.

Introduction

Synthetic glucocorticoids (Gc) are potent anti-inflammatory drugs used to treat multiple conditions including asthma and rheumatoid arthritis (Schett *et al.*, 2008;Krishnan *et al.*, 2009). Unfortunately Gc treatment also carries a wide range of serious side effects including hyperglycaemia and osteoporosis (Canalis *et al.*, 2002). In recent years a significant effort has been made to design dissociative ligands with the anti-inflammatory potency of conventional Gc, but with a reduced spectrum of side-effects (Lin *et al.*, 2002;Bledsoe *et al.*, 2004;Cerasoli, Jr., 2006;Wang *et al.*, 2006;McMaster and Ray, 2007;McMaster and Ray, 2008;van Lierop *et al.*, 2012).

Gc actions are mediated by the ubiquitously expressed glucocorticoid receptor (GR; NR3C1) a member of the nuclear hormone receptor superfamily with a conserved modular structure consisting of an N-terminal regulatory domain, a DNA binding domain (DBD) and a C-terminal ligand binding domain (LBD) (Hollenberg *et al.*, 1985;Encio and tera-Wadleigh, 1991). The unliganded GR resides in the cytoplasm in a complex with heat-shock proteins and immunophilins (Grad and Picard, 2007). Ligand binding triggers rapid activation of cytosolic kinase signalling cascades and concomitantly results in exposure of two nuclear localisation signals (NLS1, and NLS2) enabling nuclear import (Picard and Yamamoto, 1987). This is accompanied by replacement of the immunophilin FKBP51 with FKBP52 (Davies *et al.*, 2002) which associates with dynein to drive GR along microtubules (Czar *et al.*, 1994;Harrell *et al.*, 2004). The process of translocation to the nucleus post ligand binding occurs rapidly, with the majority of cellular GR being nuclear 30 minutes after treatment with 100nM Dex (Nishi *et al.*, 1999). In addition cell cycle phase is able to regulate the subcellular localisation of unliganded GR, but with far slower kinetics of nuclear accumulation (Matthews *et al.*, 2011). In the nucleus GR binds to cis-elements to activate or repress target gene expression, recruiting co-modulator proteins from distinct classes to effect chromatin remodelling, and recruitment of the basal transcriptional machinery (Ford *et al.*, 1997;Jones and Shi, 2003;Ito *et al.*, 2006;Johnson *et al.*, 2008).

GR recruits co-modulator proteins via its transcriptional activation function domains (AF1, and AF2) (Warnmark *et al.*, 2000;Kumar *et al.*, 2001;Bledsoe *et al.*, 2002). The GR AF1 is the site of various post translational modifications including

phosphorylation, both in the presence and absence of ligand. (Wang *et al.*, 2002;Ismaili and Garabedian, 2004;Galliher-Beckley *et al.*, 2008). Phosphorylation directs GR function by impacting protein stability and recruitment of specific co-modulator proteins such as MED14 (Chen *et al.*, 2006;Chen *et al.*, 2008). In addition, co-modulators bind to the GR AF2 domain, within the LBD (Heery *et al.*, 1997). Structural information about bound ligand is transmitted through differential folding of the LBD, which directs GR function by offering differentially attractive signals for co-modulator recruitment. Both GR agonists and antagonists provoke similar rapid kinetics of nuclear translocation, but differ in the profile of co-modulator proteins recruitment, providing a mechanism for their different modes of action (Bledsoe *et al.*, 2002;Kauppi *et al.*, 2003;Stevens *et al.*, 2003).

Here we identify a novel switch mechanism that regulates GR trafficking in response to ligand binding, distinct from an effect attributable to ligand potency. We identify two novel, non-steroidal GR ligands that regulate the GR surface to greatly reduce rates of nuclear translocation and reduce reliance on heat-shock protein for continuing activity. The difference in GR conformation induced by the novel GR ligands reveals a patch of positive charge on the surface of the LBD. We propose that this prevents efficient engagement with the active nuclear translocation mechanism, subsequent export, and protein degradation mechanisms for the GR. The result is generation of ligands with greatly prolonged duration of action as a consequence of altered pharmacodynamics rather than pharmacokinetics.

Materials and methods

Anti-hGR (clone 41, BD Biosciences, Oxford, UK); Anti-phospho-(Ser211)-GR, anti αTubulin (Cell Signalling Technology, MA, USA); Horseradish peroxidase conjugated anti-mouse and anti-rabbit (GE Healthcare, Buckinghamshire, UK); Dexamethasone, Hydrocortisone and Fluticasone Propionate (Sigma, Dorset, UK). TAT3-Luciferase, and NRE-luciferase have been previously described (Matthews *et al.*, 2008;Matthews *et al.*, 2009).

Cell culture and maintenance

HeLa cells and A549 cells (ATCC, Teddington, UK) were cultured in low glucose (1 g/l) Dulbecco's modified Eagle's medium (DMEM; PAA, Yeovil, UK) supplemented with stable 2 mM glutamine (PAA) and 10 % heat inactivated fetal bovine serum (FBS; Invitrogen, Paisley, UK) or 10 % charcoal dextran stripped fetal calf serum (sFCS; Invitrogen). A549's stably transfected with GRE-Luc and NRE-Luc were also supplemented with 1% Non essential amino acid (NEAA; Invitrogen) and 1% Geneticin (Invitrogen). All cells were grown in a humidified atmosphere of 5 % carbon dioxide at 37 ^{o}C.

Immunoblot analysis

Following treatment cells were lysed in RIPA buffer (50 mM TrisCl pH7.4, 1 % NP40 (Igepal), 0.25 % Na-deoxycholate 150 mM NaCl, 1 mM EDTA) containing protease and phosphatase inhibitors (Sigma), and 10 μg protein was electrophoresed on Tris/Glycine 4-12 % gels (Invitrogen) and transferred to 0.2 micron nitrocellulose membranes (BioRad Laboratories, Hertfordshire, UK) overnight at 4 °C. Membranes were blocked for 2 hours (NaCl 0.15 M, 2 % dried milk, 0.1 % Tween 20) and incubated with primary antibodies (diluted in blocking buffer) overnight at 4 ˚C. After three 10 minute washes (88 mM Tris pH 7.8, 0.25 % dried milk, 0.1 % Tween 20), membranes were incubated with a species-specific horseradish peroxidase-conjugated secondary antibody (diluted in wash buffer) for 1 hour at room temperature, and washed a further three times, each for 10 minutes. Immunoreactive proteins were visualised using enhanced chemiluminescence (ECL Advance, GE Healthcare).

Reporter gene assays

HeLa cells seeded in DMEM containing sFCS were co-transfected with 2 μg reporter gene and 0.5 μg CMV-renilla luciferase (to correct for transfection efficiency) using Fugene 6 (Roche Diagnostics, West Sussex, UK) at a ratio of 3:1 (v/w). 24 hours post transfection, cells were treated as specified in results prior to lysis, then assayed for luciferase activity using a dual-luciferase reporter assay system following the manufacturer's instructions (Promega, Southampton, UK).

Stable A549 GRE-Luc or NRE-Luc cells were seeded in DMEM containing sFCS into 96 well plates and incubated overnight. Cells were treated as specified in results and 18 hours later each well washed twice with PBS (first without Mg^{2+}, Ca^{2+}, then with Mg^{2+}, Ca^{2+}). Renilla Glo (Promega, E2720) or Bright Glo (Promega E2620) lysis buffer was added the GRE cells or the NRE cells respectively according to the manufacturer's instructions. Cell lysates were read using a luminometer (Wallac 1450 MicroBeta Trilux Liquid Scintillation counter and luminometer). Ten one second reads were taken per well and the average RLU determined.

Immunofluorescence

Fixed cells: Following 24 hours in DMEM containing sFCS, HeLa cells were transfected (Fugene 6) with hGR-GFP and treated as specified in results. Cells were fixed with 4 % paraformaldehyde for 30 minutes at 4 ˚C, and subsequently stained with Hoeschst (Sigma) in PBS (2 μg/ml) for 20 minutes at 4 ˚C. Following three 5 minute washes in PBS, coverslips were mounted using Vectamount AQ (Vector Laboratories, Peterborough, UK). Images were acquired on a Delta Vision RT (Applied Precision, GE Healthcare) restoration microscope using a 40X/0.85 Uplan Apo objective and the Sedat Quad filter set (Chroma 86000v2, VT, USA). The images were collected using a Coolsnap HQ (Photometrics, AZ, USA) camera with a Z optical spacing of 0.5μm. Raw images were then deconvolved using the Softworx software (GE Healthcare) and average intensity projections of these deconvolved images processed using Image J (Rasband, 1997).

Live cells: Following 24 hours in DMEM containing sFCS, HeLa cells were transfected (Fugene 6) with 5μg GR-GFP and transferred to a glass bottomed 24 well plates. Alternatively HeLa cells were plated into a glass bottomed 24 well plate in

DMEM containing sFCS. Each well was transfected (Fugene 6) with 0.5μg HaloTag-GR (Catalog number FHC10483, Promega) and incubated for 16 hours with 0.25μl Halo ligand (HaloTag TMRDirect, Catalog number G2991, Promega) to enable visualisation. Subcellular GR trafficking was tracked in real time at 37^{o}C with 5% CO_2. Images were acquired on a Nikon TE2000 PFS microscope using a 60x/ 1.40 Plan Apo or 40x/1.25 Plan Apl objective and the Sedat filter set (Chroma 89000). The images were collected using a Cascade II EMCCD camera (Photometrics). Raw images were then processed using Image J.

Fluorescent recovery after photobleaching (FRAP)

HeLa cells were transfected (Fugene 6) with 5 μg hGR-GFP then seeded into a glass bottomed 24 well plate. Cells were maintained at 37^{o}C and 5% CO_2 and images collected on a Leica TCS SP5 AOBS inverted confocal (Leica, Milton Keynes, UK) using a 63x/ 0.50 Plan Fluotar objective and 7x confocal zoom. The confocal settings were as follows, pinhole 1 airy unit, scan speed 1000Hz unidirectional, format 1024 x 1024. Images were collected using the following detection mirror settings; FITC 494-530nm using the 488nm (13%).

MTS Assay

Cells were seeded into a 96 well plate were treated as described in the results. Upon completion of the treatment 10 μl of MTS reagent (Promega) was added to each well. Cells were incubated for 4 hours, reading at 490nm every hour.

Q-RTPCR

Cells were treated as required, then lysed and RNA extracted using an RNeasy kit (Qiagen). 10 ng RNA was reverse transcribed, and subjected to qPCR using Sybr Green detection in an ABI q-PCR machine (Applied biosystems, CA, USA) and data analysed by δδCT method (Livak and Schmittgen, 2001).

Bioluminescence real-time recording

HeLa cells transfected (Fugene 6) with 2μg TAT3-luc plasmid were grown to 80% confluency in 35-mm tissue culture dishes in phenol red free DMEM with 10% FCS and 1% glutamine. Prior to the experiment, cells were supplemented with 0.1 mM

Luciferin substrate (Izumo *et al.*, 2003;Yamazaki and Takahashi, 2005). Each dish lid was replaced with a glass cover then sealed with vacuum grease before being placed in a light-tight and temperature-controlled (37°C) environment. Light emission (bioluminescence) was measured continuously using a Photomultiplier tube (PMT, H6240 MOD1, Hamamatsu Photonics, Hertfordshire, UK). Baseline measurements (photon counts per minute) were taken for each PMT prior to treatment and then deducted from the experimental values attained.

Measurement of ligand uptake using mass spectroscopy

A549 cells were grown to 90% confluency in 6 well plates. Following treatment the media was removed from the cells and retained for analysis. The cells were washed three times with PBS and lysed in 300µl of M-Per mammalian protein extraction reagent (#78503, Thermoscientific, Essex, UK) on the shaker at 750rpm at room temperature for 5 minutes. The whole cell lysate was collected, then centrifuged at 10000rpm for 10 minutes, then the supernatant collected and analysed by mass spectrometry.

Measurement of cytokine production

A549 cells were seeded into a 96 well plate into DMEM with 10% FCS and incubated overnight. In order to slow cell proliferation and prevent any interference from steroid present in FCS the media was changed to DMEM with 1% sFCS prior to ligand treatment. Following treatment supernatents were collected and assayed for IL6 and IL8 concentration using a Luminex 100 (Merck Millipore, MA, USA) with StarStation software according to the manufacturer's instructions.

Computational modelling of GR crystal structure

Crystal structures of GR bound to Dex (1M2Z) and GSK47866A (3E7C) (Madauss *et al.*, 2008) were downloaded from the RCSB Protein Data Bank (PDB) (Berman *et al.*, 2007). The structures were imported into Maestro (Schrodinger, 2012) and prepared using the Protein Preparation module. Each Ligand was extracted and scrambled conformationally before docking back into the native active site models to verify that the docking program (GLIDE) (Schrodinger, 2009) was competent at reproducing the x-ray pose for each complex.

Models of compounds GSK47866A, GSK47867A and GSK47869A (S-isomers) were prepared using the Ligprep module and a set of 272 conformers generated using the confgen module of Maestro. This set of conformers was docked in the 3E7C active site model yielding 62 successful poses. Again, as found in the bootstrapping exercise, GSK47866A best scoring pose was extremely close in conformation and position within the active site pocket (RMSD ~0.2), indicative of a robust model.

Crystal structures 1M2Z and 3E7C were superposed and conformations of residues within 6 Angstrom of the Dex ligand in 1M2Z were compared visually. Any differing substantially were coloured differently (Fig. 2A, B), and these atom colours projected onto a molecular surface to reveal regions of the protein surface impacted by the residue movements induced by binding of GSK47866A (Fig. 3A,C). The regions of surface modification thus highlighted guided where to look for differences in electrostatic potential, projected onto the same molecular surface (Fig. 3B,D)

Modelling of GR mutant with impaired HSP90 interaction

The original 1M2Z x-ray coordinates, already optimised for use with the OPLS forcefield in Maestro, were used to mutate M604 to Threonine. The built-in residue mutation building tool was employed for this. The mutated structure was optimised using the Protein Preparation Wizard option to perform a restrained, all-atom minimisation. Surface and electrostatic potential colouring was calculated as for all other examples, ensuring a consistent range of electrostatic potential values of -0.2 to 0.2 for the blue-white-red colour ramp.

Results

GSK47867A and GSK47869A, are highly potent GR agonists

There is wide interest in understanding how variation in ligand structure (Fig. 1A) affects the function of GR. Here, we use novel, non-steroidal glucocorticoid receptor ligands (NSG) with very high potency, and specificity for GR to determine how ligand structure impacts receptor function (Fig. 1, B-C Fig. S1). Transient GR transactivation and transrepression models in HeLa cells were used initially to compare the NSGs to conventional synthetic Gc ligands. We find that both GSK47867A and GSK47869A were approximately 30 times more potent that Dexamethasone (Dex, Fig. 1B-C, table 1). Similar results were also obtained using A549 cells with stably integrated GRE-Luc or NFκB-Luc templates (Fig. S2A-B). The steroidal Gc Fluticasone Propionate (FP) had similar potency to GSK47867A and GSK47869A. Hydrocortisone was significantly less potent than all the synthetic ligands tested (Fig. 1).

To rationalise subsequent matched analyses, saturating concentrations of the ligands were selected, calculated as 10 times the measured EC50 for transactivation (Table 1). At these concentrations all ligands showed similar repression of IL6 and IL8 secretion (Fig. S2C-D), and inhibition of cell proliferation (Fig. S2E-F).

GR crystal structure reveals ligand-specific altered surface charge

To identify conformational differences in the GR ligand binding domain (LBD), we first compared the structures of GR-Dex (1M2Z) and GR-GSK47866A (3E7C) a non-steroidal GR ligand similar in structure to GSK47867A (Figs 1A, 2). An active site model derived from the coordinates of deposited structure 3E7C was used to dock GSK47867A and GSK47869A. Both GSK47867A and GSK47869A are similar to GSK47866A and gave very high scoring fits in the binding pocket formed by GSK47866A bound to the GR LBD (Fig. S3). Inspection of the poses showed sensible, well fitting conformers, indicating that structure 3E7C was a suitable surrogate to compare with 1M2Z.

Observation of the ligand binding pocket in each crystal structure revealed that amino acids in closest proximity to each ligand demonstrated significant movement compared to Dex at the head (A ring, Fig. 2C-D) and tail (D ring, Fig. S4C-D). The

greatest displacement was seen in amino acids Gln570 and Arg611 (Fig. 2C-D). Less displacement was seen at the opposite end of the ligand; most noticeable here was the movement of Gln642 (Fig. S4C-D). The effect of residue movements in the GR LBD upon binding of GSK47866A was examined by visualisation of the molecular surface (Fig. 3, Fig. S5 and S6). This revealed a distinct surface electrostatic potential difference, highlighting a patch of positive charge in the GR-GSK47866A structure resulting from displacement of Arg611 (Fig. 3 B,D). This demonstrates that the structural difference between Dex and the NSGs results in a different GR surface charge upon binding, with potential for altered for protein-protein interactions.

NSG induce different kinetics of endogenous Gc target gene regulation

To determine whether the alteration in GR surface charge upon binding NSG had any functional consequence, transcript levels of endogenous Gc induced (GILZ and FKBP5) and Gc repressed (IL6 and IL8) target genes were quantified at multiple time points (Fig. 4A-B, Fig. S7A-B). Both the steroidal and NSG ligands displayed equivalent kinetics of FKBP5 induction (Fig. 4A). Although NSG treatment did not induce GILZ transcript at 1 hour, similar induction was observed at later time points (Fig. 4B). Similarly NSG treatment did not repress IL6 or IL8 transcripts at 1 hour but comparable repression was observed at later time points (Fig. S7A-B).

NSG treatment results in delayed kinetics of GR 211 phosphorylation

Transactivation of IGFBP1 is reliant on Ser211 phosphorylation of the GR, a signal to recruit the co-activator protein MED14. Dex treatment resulted in significant induction of IGFBP1 transcript by 1 hour (Fig. S8A), but the NSG ligands failed to induce transcript at this early time point. This lack of transcript regulation at an early time point was similarly seen with GILZ, IL6 and IL8. Ligand induction of GR Ser211 phosphorylation was compared. Treatment with Dex resulted in rapid phosphorylation of GR at both serine residues 203 and 211 (Fig. S8B). The NSG ligands induced slower onset of phosphorylation of both serine residues 203 and 211 (Fig. S8B).

NSG treatment results in slow rate of GR nuclear translocation

The delay in endogenous gene transactivation and receptor phosphorylation seen with NSG treatment suggested that nuclear translocation may also be delayed. Use of a

halo tagged GR clearly demonstrated a slower rate of nuclear translocation with both GSK47867A and GSK47869A (Fig. 4C). Ligand-bound nuclear GR has a signature FRAP signal, with reduced intranuclear mobility resulting in delayed recovery from photobleaching. FRAP studies revealed that at 1 hour following NSG treatment nuclear GR displayed characteristics of an unliganded receptor (Fig. S9A-B). However with 4 hour NSG treatment nuclear GR displayed the typical signature of liganded receptor, indicative of a delay in adoption of the activated GR conformation (Fig. S9C-D).

Altered kinetics of GR phosphorylation may explain the observed differences in nuclear translocation rate and transactivation of endogenous Gc target genes. Therefore, we made GR mutants Ser211Ala (phosphodeficient) and Ser211Asp (phosphomimetic) to assess the importance of this phosphorylation site (Fig. S10A). However, the phosphomimetic GR did not significantly increase the rate of GR translocation with either GSK47867A or GSK47869A treatment (Fig. S10C-D). Likewise the phosphodeficient GR had no significant impact on the rate of translocation seen with Dex treatment (Fig. S10B, D).

NSG treatment results in slower onset of GR transactivation

Treatment with NSG results in slowed GR nuclear translocation and delayed transactivation of endogenous Gc target genes. To measure the kinetics of GR transactivation more precisely, real-time luciferase analysis was used (Meng *et al.*, 2008;McMaster *et al.*, 2008) (Fig. 4D). This revealed that the NSG ligands consistently took longer to reach half-maximal transactivation compared to either Dex, or the higher potency FP (Fig. 4E). Interestingly all three high potency ligands resulted in greater maximal transactivation (Fig. 4D).

Delayed action of NSG ligands cannot be explained by impaired cellular uptake

One possible explanation for these observations is altered ligand access to the intracellular GR. Initially mass spectroscopy analysis of cell lysates was performed after 10 minutes ligand exposure (Fig. 5A). A 10μM concentration of each ligand was compared, to permit detection of the ligand by mass spectrometry in cell lysates. Strikingly, the NSG ligands showed greater than 10 fold increased concentrations within the cells compared to Dex, effectively ruling out delayed ligand penetration.

To further evaluate cell pharmacokinetics, cells were incubated with 100 nM Dex or 3 nM FP, GSK47867A or GSK47869A for 10 minutes, washed and then incubated in ligand-free medium for 4 hours. These samples were compared to cells treated with ligand continuously for 4 hours (Fig. 5B-D). Short exposure to both NSG ligands resulted in greater induction of GILZ and FKBP5 although not IGFBP1 compared to Dex, again demonstrating rapid cellular accumulation of ligand. Furthermore cells incubated with NSG on ice for 1 hour to permit ligand access in the absence of GR activation still showed delayed nuclear translocation (Fig. 5E-F), implicating a post receptor mechanism of action. The observed differences could not be attributed to Dex activation of mineralocorticoid receptor, as the mineralocorticoid receptor antagonist Spironolactone did not affect the Dex induction (Fig. S11A-B).

NSG bound GR shows prolonged nuclear retention

As treatment with both NSG ligands results in delayed nuclear translocation, we investigated whether nuclear export of GR may also be slower. To measure GR export HeLa cells were treated with 100 nM Dex or 3 nM NSGs for 1 hour then washed and placed in serum free media and imaged over 24 hours (Fig. S12A). In cells treated with NSG the GR-GFP was not exported from the nucleus during the 24 hour wash-out period, but Dex treated cells exported GR from the nucleus within 6 hours (Fig. S12B).

Structural modelling suggests that NSGs modify the HSP90 interaction surface

Our data clearly demonstrates that when bound to NSG there is altered interaction of GR with the translocation machinery resulting in delayed nuclear import, delayed transcriptional activity and receptor export. The chaperone heat shock protein 90 (HSP90) is known to play key roles in this aspect of GR biology, including maintaining GR structure, ligand binding activity, and trafficking of GR between nucleus and cytoplasm (Segnitz and Gehring, 1997;Tago *et al.*, 2004;Kakar *et al.*, 2006;Grad *et al.*, 2007;Echeverria *et al.*, 2009). GR residues identified by Ricketson and co-workers (Ricketson *et al.*, 2007) as important for HSP90 interaction were mapped onto the crystal structure of GR bound to Dex (Fig. 6A). Surface map analysis of GR following replacement of Met604 with Thr604, which has been shown to inhibit HSP90 recruitment, was in the same part of the GR structure that was differentially affected by NSG binding (Fig. 6B, C).

Microtubule disruption improves nuclear translocation rate

HSP90 anchors the GR to the microtubule network, so permitting rapid, energy-dependent nuclear translocation. HSP90 antagonism slows the rate of nuclear translocation (Galigniana *et al.*, 1998). However, in addition, GR can translocate using a diffusion mechanism (Nishi *et al.*, 1999). Disruption of the microtubule network using colcemid restores rapid GR translocation even in the presence HSP90 inhibitor geldanamycin (Segnitz *et al.*, 1997;Galigniana *et al.*, 1998). Therefore, we used colcemid to determine if the microtubule architecture was slowing NSG mediated nuclear translocation. Colcemid significantly increased the rate of NSG-driven nuclear translocation, but had no effect on that promoted by Dex (Fig. 6D-G), suggesting a diffusion mechanism for translocation

NSGs mediate prolonged duration of action

The duration of ligand-dependent activity depends on continuing presence of ligand, and maintaining GR in a ligand-binding compatible conformation. To investigate these phenomena we initially undertook washout studies, using real time reporter gene luciferase analysis. These revealed a striking prolongation of transactivation following NSG ligand withdrawal compared to either Dex or FP, which was not explained by increased ligand potency (Fig. 7A).

To corroborate these observations with endogenous genes a two hour ligand exposure was chased with a 24 hour washout before measurement of GILZ and FKBP5 transcripts (Fig 7B-C). There was significantly enhanced preservation of transactivation seen with both the NSGs compared to the potency matched control steroid FP.

To determine the role of HSP90 in mediating prolonged GR transactivation, geldanamycin was used. As HSP90 activity is required for initial GR ligand binding, these studies were performed sequentially, adding geldanamycin after ligand activation. The geldanamycin was added to cells at the time of maximal transactivation, in the presence of continuing ligand exposure (Fig. 7D). Both FP and Dex showed exponential decay of transactivation, as predicted. However, the NSG ligands showed a striking biphasic response, with initial potentiation, followed by decay (Fig. 7D).

As HSP90 is also essential for maintaining GR protein stability investigation of receptor abundance and phosphorylation was undertaken. Inhibition of HSP90 preserves GR protein levels following Dex treatment for 4 hours (Fig. 7E), but not at a later time point (Fig. 7F). Strikingly, the NSG ligands did not show such a ligand-dependent loss of GR protein (Fig. 7E,F), again identifying differences in HSP90 interaction with the novel NSGs. Additionally treatment of cells with Dex in the presence of geldanamycin results marked dephosphorylation of GR at serine 211 (Fig. 7E). However treatment with the NSG was protective for serine 211 phosphorylation (Fig. 7E). Collectively, these studies suggest that GR-HSP90 interactions can be modulated by ligand structure, to influence the properties of the Gc response.

Discussion

Understanding how the GR interprets its ligands to permit appropriate cellular responses is of vital interest in both physiology and pharmacology, as the GR remains an important drug target in inflammation and malignancy (Barnes, 2011;De *et al.*, 2011). The advent of drug design based on the crystal structure predicted pharmacophore has permitted new generations of ligands to be synthesised, including those studied here (Kauppi *et al.*, 2003;Bledsoe *et al.*, 2004). Our initial findings identified that although highly potent, the NSG ligands surprisingly result in slowed kinetics of GR phosphorylation, nuclear import and delayed onset of GR-dependent gene transactivation. Our data suggests that the NSG ligands fundamentally alter the mechanism of GR activation.

A possible explanation for the delayed kinetics of cellular response to GSK47867A and GSK47869A is reduced efficiency of cellular uptake of ligand. Although the NSGs retain the highly lipophilic characteristics of steroidal ligands, they may interact differentially with membrane components. However our mass spec studies in fact showed an accelerated ligand accumulation with the NSGs compared to Dex. We also undertook a functional assay, washing off ligand after a short incubation, and tracking response of Gc target genes. Again, the NSGs produced enhanced target gene transactivation compared with Dex, indicating rapid ligand accumulation. Furthermore treatment of cells with ligand for 1 hour on ice allowed for saturation of the receptor without translocation. When the cells were returned to 37^{o}C the GR rapidly translocated with both Dex and FP but translocation was slower for both the NSG ligands, supporting defective interaction with the nuclear translocation machinery post ligand binding.

To explain these observations we interrogated the crystal structure of GR LBD bound to GSK47867A and GSK47869A. This revealed a very similar conformation to that seen with Dex, but there was single difference, namely the addition of a patch of positive charge on the external surface of the LBD. Ricketson and co-workers were able to demonstrate, through amino acid substitution, that this surface is required for HSP90 interaction (Ricketson *et al.*, 2007). HSP90 recognises the GR LBD through two, defined hydrophobic sites and binds to a solvent accessible major groove maintaining GR stability and permitting high-affinity ligand binding (Fang *et al.*,

2006), as depicted in Fig. 7G. Following ligand binding HSP90 undergoes a conformation change to bind to the same region of the GR LBD, but with a different motif. This is required to couple the GR to the dynein active transport mechanism through the bridging effect of immunophilins (Harrell *et al.*, 2004)(Fig. 7G). HSP90 remains associated with the GR in the nucleus, where binding to the major groove of the GR LBD competes with recruitment of co-activators (Caamano *et al.*, 1998;Kang *et al.*, 1999;Fang *et al.*, 2006), and also promotes nuclear retention (Tago *et al.*, 2004;Kakar *et al.*, 2006). Binding of NSGs to the GR LBD forces the movement of Arg611, leading to the creation of a novel interaction surface which could be the mechanism by which interaction with HSP90 is altered. Therefore, we measured the impact of HSP90 manipulation on GR function with both the steroidal ligands, and NSGs.

GR is anchored to the microtubule network through interaction with HSP90 to facilitate nuclear translocation. Antagonism of HSP90 therefore reduces the rate of GR nuclear translocation and can be overcome by disrupting the microtubule network (Galigniana *et al.*, 1998;Nishi *et al.*, 1999). Here we show that the absence of an intact microtubule network significantly increases the rate of GR translocation in response to the NSGs but not Dex, which suggests an impaired interaction of GR-NSG with HSP90. Evidence has emerged that persisting Gc action requires cycles of dissociation, and re-binding of ligand to the GR, which occurs in a HSP90 dependent manner (Stavreva *et al.*, 2004;Conway-Campbell *et al.*, 2011)(Fig. 7G). To test the role of HSP90 we used the inhibitor geldanamycin (Segnitz *et al.*, 1997). As predicted, geldanamycin curtailed the Gc transcriptional response rapidly, irrespective of ligand potency, for the two steroid agonists. However, in keeping with the hypothesis that HSP90 binding was disrupted by the final conformation adopted by the NSG bound GR there was greatly prolonged transactivation observed, with a gradual decay likely due to degradation of GR protein. It was, however, striking that the pattern of response for both NSGs included an initial augmentation of response, which is compatible with displacement of HSP90 from the major groove, and subsequent promotion of co-activator recruitment. It is also possible that disruption of the HSP90 interaction surface also affects interaction between GR, and co-modulator protein partners (Caamano *et al.*, 1998;Kang *et al.*, 1999;Fang *et al.*, 2006).

Altered NSG-driven nuclear translocation, and interaction with HSP90 may also affect GR nuclear export, and the duration of cellular response. Indeed, our washout studies showed a dramatic difference between the steroidal and NSG ligands, with marked reduction in GR export rate and prolongation of action seen with the NSGs, observed with both transfected reporter genes, and endogenous gene transcripts. A similar prolongation of action was seen in cells treated with geldanamycin which may result from stabilised GR-ligand interaction, due to altered engagement with HSP90, and its associated protein complex, including enzymes such as protein phosphatase 5 (PP5). PP5 is responsible for removing phosphate modification from GR Ser211, and promoting GR nuclear export (DeFranco *et al.*, 1991;Silverstein *et al.*, 1997;Galigniana *et al.*, 2002;Hinds, Jr. and Sanchez, 2008)(Fig. 7G).

Geldanamycin treatment resulted in loss of the Dex ligand-dependent GR Ser211 phosphorylation. However NSG-liganded GR was not dephosphorylated under the same conditions, implying altered recruitment of PP5. PP5 also associates with HSP90 as part of the chaperone complex (Silverstein *et al.*, 1997;Hinds, Jr. *et al.*, 2008) (Fig. 7G), and contains a peptidylprolyl isomerase domain that is capable of dynein interaction and therefore forming a bridge between the GR and the nuclear export machinery (DeFranco *et al.*, 1991;Galigniana *et al.*, 2002)(Fig. 7G). Therefore, as PP5 has been implicated in the nuclear export of the GR, the lack of dephosphorylation seen with NSG treatment is compatible with a broader change in protein recruitment with the NSG ligands. Interestingly, it was also observed that NSG treatment preserved GR protein expression compared with Dex treatment. This would further suggest that the conformation adopted by GR following NSG binding decouples protein recruitment required for terminating the GR transcriptional signal (Nawaz and O'Malley, 2004)(Fig 7G).

In conclusion we have identified two NSGs that bind to GR with high specificity but paradoxically result in profoundly slowed kinetics of cellular response. Analysis of the structural effects of these NSGs bound to GR suggests a change to the GR surface, through the movement of Arg611 in the ligand binding pocket of the GR, resulting in an alteration in the GR surface charge. The change in electrostatic charge is close to the known binding site for HSP90, and co-modulator proteins. This alteration carries with it the consequence of delayed GR phosphorylation and nuclear translocation,

which in turn results in delayed early Gc target gene regulation. The ability to manipulate the kinetics of GR activation by designing novel NSGs has implications for therapy, by targeting cellular pharmacodynamics rather than organismal pharmacokinetics.

Acknowledgements

We thank Bill Leavens and Midori Kayahara for technical assistance. Special thanks to Peter March and Roger Meadows for their help with the microscopy. Peter Trebble is supported by a BBSRC CASE studentship. Laura Matthews is supported by a FMHS Stepping Stones Fellowship. The Bioimaging Facility microscopes used in this study were purchased with grants from BBSRC, Wellcome and the University of Manchester Strategic Fund.

REFERENCES

Barnes PJ (2011) Glucocorticosteroids: current and future directions. *Br J Pharmacol,* 163, 29-43.

Berman H, Henrick K, Nakamura H, and Markley JL (2007) The worldwide Protein Data Bank (wwPDB): ensuring a single, uniform archive of PDB data. *Nucleic Acids Res,* 35, D301-D303.

Bledsoe RK, Montana VG, Stanley TB, Delves CJ, Apolito CJ, McKee DD, Consler TG, Parks DJ, Stewart EL, Willson TM, Lambert MH, Moore JT, Pearce KH, and Xu HE (2002) Crystal structure of the glucocorticoid receptor ligand binding domain reveals a novel mode of receptor dimerization and coactivator recognition. *Cell,* 110, 93-105.

Bledsoe RK, Stewart EL, and Pearce KH (2004) Structure and function of the glucocorticoid receptor ligand binding domain. *Vitam Horm,* 68, 49-91.

Caamano CA, Morano MI, Dalman FC, Pratt WB, and Akil H (1998) A conserved proline in the hsp90 binding region of the glucocorticoid receptor is required for hsp90 heterocomplex stabilization and receptor signaling. *J Biol Chem,* 273, 20473-20480.

Canalis E, Pereira RC, and Delany AM (2002) Effects of glucocorticoids on the skeleton. *J Pediatr Endocrinol Metab,* 15 Suppl 5, 1341-1345.

Cerasoli F, Jr. (2006) Developing the ideal inhaled corticosteroid. *Chest,* 130, 54S-64S.

Chen W, Rogatsky I, and Garabedian MJ (2006) MED14 and MED1 differentially regulate target-specific gene activation by the glucocorticoid receptor. *Mol Endocrinol,* 20, 560-572.

Chen W, Dang T, Blind RD, Wang Z, Cavasotto CN, Hittelman AB, Rogatsky I, Logan SK, and Garabedian MJ (2008) Glucocorticoid Receptor Phosphorylation Differentially Affects Target Gene Expression. *Mol Endocrinol,* 22, 1754-1766.

Conway-Campbell BL, George CL, Pooley JR, Knight DM, Norman MR, Hager GL, and Lightman SL (2011) The HSP90 molecular chaperone cycle regulates cyclical transcriptional dynamics of the glucocorticoid receptor and its coregulatory molecules CBP/p300 during ultradian ligand treatment. *Mol Endocrinol,* 25, 944-954.

Czar MJ, Owens-Grillo JK, Yem AW, Leach KL, Deibel MR, Jr., Welsh MJ, and Pratt WB (1994) The hsp56 immunophilin component of untransformed steroid receptor complexes is localized both to microtubules in the cytoplasm and to the same nonrandom regions within the nucleus as the steroid receptor. *Mol Endocrinol,* 8, 1731-1741.

600 Davies TH, Ning YM, and Sanchez ER (2002) A new first step in activation of steroid
601 receptors: hormone-induced switching of FKBP51 and FKBP52 immunophilins. *J*
602 *Biol Chem*, 277, 4597-4600.

603 De IS, Franca R, Martelossi S, Ventura A, and Decorti G (2011) Molecular
604 mechanism of glucocorticoid resistance in inflammatory bowel disease. *World J*
605 *Gastroenterol*, 17, 1095-1108.

606 DeFranco DB, Qi M, Borror KC, Garabedian MJ, and Brautigan DL (1991) Protein
607 phosphatase types 1 and/or 2A regulate nucleocytoplasmic shuttling of
608 glucocorticoid receptors. *Mol Endocrinol*, 5, 1215-1228.

609 Echeverria PC, Mazaira G, Erlejman A, Gomez-Sanchez C, Piwien PG, and
610 Galigniana MD (2009) Nuclear import of the glucocorticoid receptor-hsp90
611 complex through the nuclear pore complex is mediated by its interaction with
612 Nup62 and importin beta. *Mol Cell Biol*, 29, 4788-4797.

613 Encio IJ and tera-Wadleigh SD (1991) The genomic structure of the human
614 glucocorticoid receptor. *J Biol Chem*, 266, 7182-7188.

615 Fang L, Ricketson D, Getubig L, and Darimont B (2006) Unliganded and hormone-
616 bound glucocorticoid receptors interact with distinct hydrophobic sites in the
617 Hsp90 C-terminal domain. *Proc Natl Acad Sci U S A*, 103, 18487-18492.

618 Ford J, McEwan IJ, Wright AP, and Gustafsson JA (1997) Involvement of the
619 transcription factor IID protein complex in gene activation by the N-terminal
620 transactivation domain of the glucocorticoid receptor in vitro. *Mol Endocrinol*, 11,
621 1467-1475.

622 Galigniana MD, Harrell JM, Murphy PJ, Chinkers M, Radanyi C, Renoir JM, Zhang
623 M, and Pratt WB (2002) Binding of hsp90-associated immunophilins to
624 cytoplasmic dynein: direct binding and in vivo evidence that the peptidylprolyl
625 isomerase domain is a dynein interaction domain. *Biochemistry*, 19;41, 13602-
626 13610.

627 Galigniana MD, Scruggs JL, Herrington J, Welsh MJ, Carter-Su C, Housley PR, and
628 Pratt WB (1998) Heat shock protein 90-dependent (geldanamycin-inhibited)
629 movement of the glucocorticoid receptor through the cytoplasm to the nucleus
630 requires intact cytoskeleton. *Mol Endocrinol*, 12, 1903-1913.

631 Galliher-Beckley AJ, Williams JG, Collins JB, and Cidlowski JA (2008) Glycogen
632 synthase kinase 3beta-mediated serine phosphorylation of the human
633 glucocorticoid receptor redirects gene expression profiles. *Mol Cell Biol*, 28, 7309-
634 7322.

635 Grad I and Picard D (2007) The glucocorticoid responses are shaped by molecular
636 chaperones. *Mol Cell Endocrinol*, 275, 2-12.

637 Harrell JM, Murphy PJ, Morishima Y, Chen H, Mansfield JF, Galigniana MD, and
638 Pratt WB (2004) Evidence for glucocorticoid receptor transport on microtubules by
639 dynein. *J Biol Chem*, 279, 54647-54654.

640 Heery DM, Kalkhoven E, Hoare S, and Parker MG (1997) A signature motif in
641 transcriptional co-activators mediates binding to nuclear receptors. *Nature*, 387,
642 733-736.

643 Hinds TD, Jr. and Sanchez ER (2008) Protein phosphatase 5. *Int J Biochem Cell Biol*,
644 40, 2358-2362.

645 Hollenberg SM, Weinberger C, Ong ES, Cerelli G, Oro A, Lebo R, Thompson EB,
646 Rosenfeld MG, and Evans RM (1985) Primary structure and expression of a
647 functional human glucocorticoid receptor cDNA. *Nature*, 318, 635-641.

648 Ismaili N and Garabedian MJ (2004) Modulation of glucocorticoid receptor function
649 via phosphorylation. *Ann N Y Acad Sci*, 1024, 86-101.

650 Ito K, Yamamura S, Essilfie-Quaye S, Cosio B, Ito M, Barnes PJ, and Adcock IM
651 (2006) Histone deacetylase 2-mediated deacetylation of the glucocorticoid receptor
652 enables NF-kappaB suppression. *J Exp Med*, 203, 7-13.

653 Izumo M, Johnson CH, and Yamazaki S (2003) Circadian gene expression in
654 mammalian fibroblasts revealed by real-time luminescence reporting: temperature
655 compensation and damping. *Proc Natl Acad Sci U S A*, 100, 16089-16094.

656 Johnson TA, Elbi C, Parekh BS, Hager GL, and John S (2008) Chromatin remodeling
657 complexes interact dynamically with a glucocorticoid receptor-regulated promoter.
658 *Mol Biol Cell*, 19, 3308-3322.

659 Jones PL and Shi YB (2003) N-CoR-HDAC corepressor complexes: roles in
660 transcriptional regulation by nuclear hormone receptors. *Curr Top Microbiol*
661 *Immunol*, 274, 237-268.

662 Kakar M, Kanwal C, Davis JR, Li H, and Lim CS (2006) Geldanamycin, an inhibitor
663 of Hsp90, blocks cytoplasmic retention of progesterone receptors and
664 glucocorticoid receptors via their respective ligand binding domains. *AAPS J*, 8,
665 E718-E728.

666 Kang KI, Meng X, vin-Leclerc J, Bouhouche I, Chadli A, Cadepond F, Baulieu EE,
667 and Catelli MG (1999) The molecular chaperone Hsp90 can negatively regulate the
668 activity of a glucocorticosteroid-dependent promoter. *Proc Natl Acad Sci U S A*,
669 96, 1439-1444.

670 Kauppi B, Jakob C, Farnegardh M, Yang J, Ahola H, Alarcon M, Calles K, Engstrom
671 O, Harlan J, Muchmore S, Ramqvist AK, Thorell S, Ohman L, Greer J, Gustafsson
672 JA, Carlstedt-Duke J, and Carlquist M (2003) The three-dimensional structures of
673 antagonistic and agonistic forms of the glucocorticoid receptor ligand-binding
674 domain: RU-486 induces a transconformation that leads to active antagonism. *J*
675 *Biol Chem*, 278, 22748-22754.

676 Krishnan JA, Davis SQ, Naureckas ET, Gibson P, and Rowe BH (2009) An umbrella
677 review: corticosteroid therapy for adults with acute asthma. *Am J Med*, 122, 977-
678 991.

679 Kumar R, Lee JC, Bolen DW, and Thompson EB (2001) The conformation of the
680 glucocorticoid receptor af1/tau1 domain induced by osmolyte binds co-regulatory
681 proteins. *J Biol Chem,* 276, 18146-18152.

682 Lin CW, Nakane M, Stashko M, Falls D, Kuk J, Miller L, Huang R, Tyree C, Miner
683 JN, Rosen J, Kym PR, Coghlan MJ, Carter G, and Lane BC (2002) trans-
684 Activation and Repression Properties of the Novel Nonsteroid Glucocorticoid
685 Receptor Ligand 2,5-Dihydro-9-hydroxy-10-methoxy-2,2,4-trimethyl-5-(1-
686 methylcyclohexen-3-y1)-1H-[1]benzopyrano[3,4-f]quinoline (A276575) and Its
687 Four Stereoisomers. *Mol Pharmacol,* 62, 297-303.

688 Livak KJ and Schmittgen TD (2001) Analysis of relative gene expression data using
689 real-time quantitative PCR and the 2(-Delta Delta C(T)) Method. *Methods,* 25,
690 402-408.

691 Madauss KP, Bledsoe RK, Mclay I, Stewart EL, Uings IJ, Weingarten G, and
692 Williams SP (2008) The first X-ray crystal structure of the glucocorticoid receptor
693 bound to a non-steroidal agonist. *Bioorg Med Chem Lett,* 18, 6097-6099.

694 Matthews L, Berry A, Ohanian V, Ohanian J, Garside H, and Ray D (2008) Caveolin
695 Mediates Rapid Glucocorticoid Effects and Couples Glucocorticoid Action to the
696 Antiproliferative Program. *Mol Endocrinol,* 22, 1320-1330.

697 Matthews L, Berry A, Tersigni M, D'Acquisto F, Ianaro A, and Ray D (2009)
698 Thiazolidinediones Are Partial Agonists for the Glucocorticoid Receptor.
699 *Endocrinology,* 150, 75-86.

700 Matthews L, Johnson J, Berry A, Trebble P, Cookson A, Spiller D, Rivers C, Norman
701 M, White M, and Ray D (2011) Cell cycle phase regulates glucocorticoid receptor
702 function. *PLoS One,* 6, e22289.

703 McMaster A, Chambers T, Meng QJ, Grundy S, Loudon AS, Donn R, and Ray DW
704 (2008) Real-time analysis of gene regulation by glucocorticoid hormones. *J*
705 *Endocrinol,* 197, 205-211.

706 McMaster A and Ray DW (2007) Modelling the glucocorticoid receptor and
707 producing therapeutic agents with anti-inflammatory effects but reduced side-
708 effects. *Exp Physiol,* 92, 299-309.

709 McMaster A and Ray DW (2008) Drug Insight: selective agonists and antagonists of
710 the glucocorticoid receptor. *Nat Clin Pract End Met,* 4, 91-101.

711 Meng QJ, McMaster A, Beesley S, Lu WQ, Gibbs J, Parks D, Collins J, Farrow S,
712 Donn R, Ray D, and Loudon A (2008) Ligand modulation of REV-ERBalpha
713 function resets the peripheral circadian clock in a phasic manner. *J Cell Sci,* 121,
714 3629-3635.

715 Nawaz Z and O'Malley BW (2004) Urban renewal in the nucleus: is protein turnover
716 by proteasomes absolutely required for nuclear receptor-regulated transcription?
717 *Mol Endocrinol,* 18, 493-499.

718 Nishi M, Takenaka N, Morita N, Ito T, Ozawa H, and Kawata M (1999) Real-time
719 imaging of glucocorticoid receptor dynamics in living neurons and glial cells in
720 comparison with non-neural cells. *Eur J Neurosci,* 11, 1927-1936.

721 Picard D and Yamamoto KR (1987) Two signals mediate hormone-dependent nuclear
722 localization of the glucocorticoid receptor. *EMBO J,* 6, 3333-3340.

723 Rasband WS. Image J. 1997. National Institutes of Health, Bethesda, Maryland,
724 USA. 1997.
725 Ref Type: Computer Program

726 Ricketson D, Hostick U, Fang L, Yamamoto KR, and Darimont BD (2007) A
727 conformational switch in the ligand-binding domain regulates the dependence of
728 the glucocorticoid receptor on Hsp90. *J Mol Biol,* 368, 729-741.

729 Schett G, Stach C, Zwerina J, Voll R, and Manger B (2008) How antirheumatic drugs
730 protect joints from damage in rheumatoid arthritis. *Arthritis Rheum,* 58, 2936-
731 2948.

732 Schrodinger. Glide version 5.5. 2009. New York, NY, Schrodinger LLC.
733 Ref Type: Computer Program

734 Schrodinger. Maestro version 9.3. 2012. New York, NY, Schrodinger LLC.
735 Ref Type: Computer Program

736 Segnitz B and Gehring U (1997) The function of steroid hormone receptors is
737 inhibited by the hsp90-specific compound geldanamycin. *J Biol Chem,* 272,
738 18694-18701.

739 Silverstein AM, Galigniana MD, Chen MS, Owens-Grillo JK, Chinkers M, and Pratt
740 WB (1997) Protein phosphatase 5 is a major component of glucocorticoid
741 receptor.hsp90 complexes with properties of an FK506-binding immunophilin. *J*
742 *Biol Chem,* 272, 16224-16230.

743 Stavreva DA, Muller WG, Hager GL, Smith CL, and McNally JG (2004) Rapid
744 glucocorticoid receptor exchange at a promoter is coupled to transcription and
745 regulated by chaperones and proteasomes. *Mol Cell Biol,* 24, 2682-2697.

746 Stevens A, Garside H, Berry A, Waters C, White A, and Ray D (2003) Dissociation of
747 steroid receptor coactivator 1 and nuclear receptor corepressor recruitment to the
748 human glucocorticoid receptor by modification of the ligand-receptor interface: the
749 role of tyrosine 735. *Mol Endocrinol,* 17, 845-859.

750 Tago K, Tsukahara F, Naruse M, Yoshioka T, and Takano K (2004) Regulation of
751 nuclear retention of glucocorticoid receptor by nuclear Hsp90. *Mol Cell*
752 *Endocrinol,* 213, 131-138.

753 van Lierop MJ, Alkema W, Laskewitz AJ, Dijkema R, van der Maaden HM, Smit MJ,
754 Plate R, Conti PG, Jans CG, Timmers CM, van Boeckel CA, Lusher SJ, McGuire
755 R, van Schaik RC, de VJ, Smeets RL, Hofstra CL, Boots AM, van DM, Ingelse
756 BA, Schoonen WG, Grefhorst A, van Dijk TH, Kuipers F, and Dokter WH (2012)
757 Org 214007-0: a novel non-steroidal selective glucocorticoid receptor modulator

with full anti-inflammatory properties and improved therapeutic index. *PLoS One*, 7, e48385.

Wang JC, Shah N, Pantoja C, Meijsing SH, Ho JD, Scanlan TS, and Yamamoto KR (2006) Novel arylpyrazole compounds selectively modulate glucocorticoid receptor regulatory activity. *Genes Dev*, 20, 689-699.

Wang Z, Frederick J, and Garabedian MJ (2002) Deciphering the phosphorylation "code" of the glucocorticoid receptor in vivo. *J Biol Chem*, 277, 26573-26580.

Warnmark A, Gustafsson JA, and Wright AP (2000) Architectural principles for the structure and function of the glucocorticoid receptor tau 1 core activation domain. *J Biol Chem*, 275, 15014-15018.

Yamazaki S and Takahashi JS (2005) Real-time luminescence reporting of circadian gene expression in mammals. *Methods Enzymol*, 393:288-301., 288-301.

Figure legends

Fig. 1: GSK47867A and GSK47869A are highly potent GR agonists.
Structure of steroidal and non steroidal Gc (A). HeLa cells were transfected with a positive GR reporter gene (TAT3-luc) (B) or with a glucocorticoid repressed NFκB reporter gene (NRE-luc) (C). Twenty four hours post-transfection, NRE-Luc transfected cells were pre-treated with TNF α (0.5 ng/ml) for thirty minutes. Subsequently all transfected cells were treated with 0.01-1000 nM Dex, Hydrocortisone (HC), GSK47867A [67A] or GSK47869A [69A] for eighteen hours then lysed and subjected to analysis by luciferase assay. Graph (mean ± SD) show the relative light units (RLU) (B) or % inhibition (C) from one of three representative experiments performed in triplicate.

Fig. 2: Dex and GSK47867A binding induces different GR LBD structure.
Comparison of the crystal structures of the GR LBD bound to Dex (A, purple) and GSK47867A [67A] (B, blue). The residues in the binding pocket that show significant movement upon 67A binding are highlighted in yellow. When 67A binds to the GR LBD the head region causes movement of residues Gln570, Met604 and Arg611 (D) when compared to Dex (C).

Fig. 3: GR LBD surface charge is altered by GSK47867A binding.
The region of the GR LBD surface where residues Gln570, Met604 and Arg611 are exposed is highlighted (A, with Dex in purple and C, GSK47867A [67A] in blue). A close up of this region is shown with an electrostatic charge map (B, D) reveals the creation of a patch of positive surface charge due to the movement of Arg611 upon 67A binding.

Fig. 4: GSK47867A and GSK47869A induce slow kinetics of GR activation.
HeLa cells were treated with DMSO vehicle, 100 nM Dex, 3 nM GSK47867A [67A] or 3 nM GSK47869A [69A] for one, four or twenty four hours then lysed and RNA extracted using an RNeasy kit. RNA was reverse transcribed and subjected to qPCR of FKBP5 (A) and GILZ (B) using Sybr Green detection in an ABI q-PCR machine and data analysed by δδ CT method. Graphs (mean ± SEM) combine data from three separate experiments and display fold change over vehicle treated control. Following transfection with HaloTag-GR HeLa cells were incubated with 100 nM Dex, 3 nM FP, 3 nM 67A or 69A. (C) Cells were imaged in real time at 37^{o}C to determine the subcellular localisation of the GR (white) at the times indicated. Scale bar, 25μm. Images are representative of three independent experiments. (D) HeLa cells transfected with a TAT3-Luc reporter plasmid were treated with 100 nM Dex, 3 nM FP, 3 nM 67A or 69A for up to twenty four hours. The production of luciferase was tracked by measuring the relative light units (RLU) emitted from each sample, graph D tracks RLU production over the first five hours following addition of treatment. Graph is representative of three separate experiments. The time taken to reach half the maximal light output was measured for all treatments (E). Statistical significance was evaluated by one way ANOVA followed by Tukey post-test. Asterisks indicate: *p < 0.005 significantly different from control, **p < 0.001 significantly different from Dex.

Fig. 5: GSK47867A and GSK47869A rapidly accumulate in cells.

A549 cells were treated with 10 μM Dex, FP, GSK47867A [67A] or GSK47869A [69A] for ten minutes and subsequently washed and lysed. The cell samples were analysed for ligand uptake by mass spectrometry (A). HeLa cells were treated with DMSO vehicle, 100 nM Dex, 3 nM 67A or 3 nM 69A either for four hours or for ten minutes followed by washout and cultured in ligand free media for four hours. Subsequently cells were lysed and RNA extracted using an RNeasy kit. RNA was reverse transcribed and subjected to qPCR of GILZ (B), FKBP5 (C) and IGFBP1 (D) using Sybr Green detection in an ABI q-PCR machine and data analysed by δδ CT method. Graphs (mean ± SEM) combine data from three separate experiments and display percentage induction compared to equivalent four hour constant treatment. Following transfection with HaloTag-GR HeLa cells were placed on ice for ten minutes and subsequently incubated with 100 nM Dex, 3 nM FP, 3 nM 67A or 69A for one hour on ice. Following treatment cells were imaged in real time at 37^{o}C to determine the subcellular localisation of the GR (white, E). Scale bar, 25μm. Graph F displays average time to exclusively nuclear GR following 1 hour with ligand on ice, calculated from three separate experiments. Statistical significance was evaluated by one way ANOVA followed by Tukey post-test. Asterisks indicate: *p < 0.001 significantly different from Dex.

Fig. 6: Mutation of Met604 in GR-LBD impairs HSP90-GR interaction and microtubule stability regulates GR translocation.
(A) The ribbon structure of the GR LBD bound to Dex. The residues highlighted in yellow were identified by Ricketson *et al* as important for GR and HSP90 interaction. The region of the GR LBD surface where the NSGs cause an alteration in surface charge is shown in panel B. The region of the GR LBD surface where Met604 is exposed is highlighted in panel C in yellow. This area overlaps the region identified as having altered surface charge upon binding NSG, supporting the lack of HSP90 engagement with NSG treatment. (D) Untreated HeLa cells with GFP labelled microtubules. Incubation for 1 hour with 2 μM colcemid disrupts the microtubule network (E). Following transfection with a halo tagged GR, Hela cells were incubated with 2 μM Colcemid for 1 hour then subsequently co treated with 100 nM Dexamethasone, 3 nM FP, GSK47867A [67A] or GSK47869A (F). Cells were imaged in real time and analysed for subcellular localisation of the GR (white). Scale bar, 25μm. Graph G shows the average time to exclusively nuclear GR. Statistical significance was evaluated by one way ANOVA followed by Tukey post-test. Asterisks indicate: * p <0.005 significantly different from treatment without colcemid

Fig. 7: Antagonism of HSP90 has less impact on the activity of NSG ligands
HeLa cells transfected with a TAT3-Luc reporter plasmid were treated with 100 nM Dex, 3 nM GSK47867A [67A] or 3 nM GSK47869A [69A] for twenty four hours. Subsequently cells were either co treated with 10 mM geldanamycin (D) or washed and placed in serum free recording media (A) for a further twenty four hours. The production of luciferase was tracked by measuring the relative light units (RLU) emitted from each sample. Graphs tracks RLU production for twenty four hours following GA addition or ligand removal. Graphs are representative of three separate experiments. HeLa cells were treated with DMSO vehicle, 100 nM Dex, 3 nM FP, 3nM 67A or 3 nM 69A for twenty four hours or one hour followed by washes and then cultured in ligand free media for twenty four hours. Subsequently cells were lysed and RNA extracted using an RNeasy kit. RNA was reverse transcribed and subjected to qPCR of GILZ (B) and FKBP5 (C) using Sybr Green detection in an ABI

q-PCR machine and data analysed by δδ CT method. Graphs (mean ± SEM) combine data from three separate experiments and display percentage induction compared to equivalent twenty four hour constant treatment. HeLa cells were treated with 100 nM Dex, 3 nM 67A or 69A for 2 hours and then co treated with 10 mM GA for a further two hours (E) or twenty two hours (F), where a constant four hour or twenty four hour treatment was used as a comparison. Following incubation with treatments cells were lysed in RIPA buffer containing phosphatase and protease inhibitors and analysed by immunoblotting for GR abundance and GR ser 211 phosphorylation. α-Tubulin was used as a loading control. Mechanism of GR action (G). Upon binding Gc (1) the GR interacts with the translocation machinery enabling nuclear import (2). In the nucleus GR binds to cis-elements to activate or repress target gene expression (3). The GR undergoes dynamic cycles of dissociation, and re-binding of ligand, which occurs in a HSP90 dependent manner (4). Interaction with PP5 facilitates nuclear export of the GR (5) enabling it to be recycled or targeted for degradation by the proteasome (6). Statistical significance was evaluated by one way ANOVA followed by Tukey post-test. Asterisks indicate: *$p < 0.01$ significantly different from both Dex and FP.

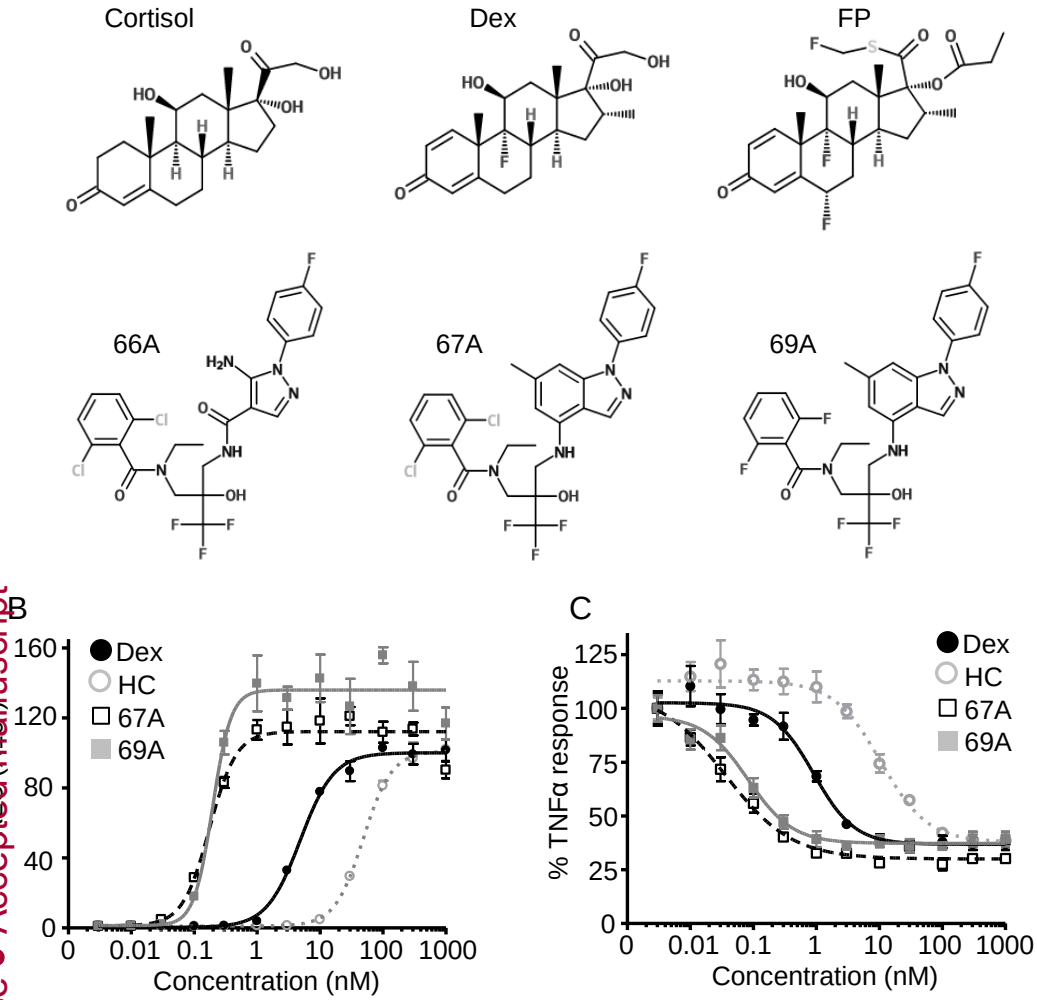

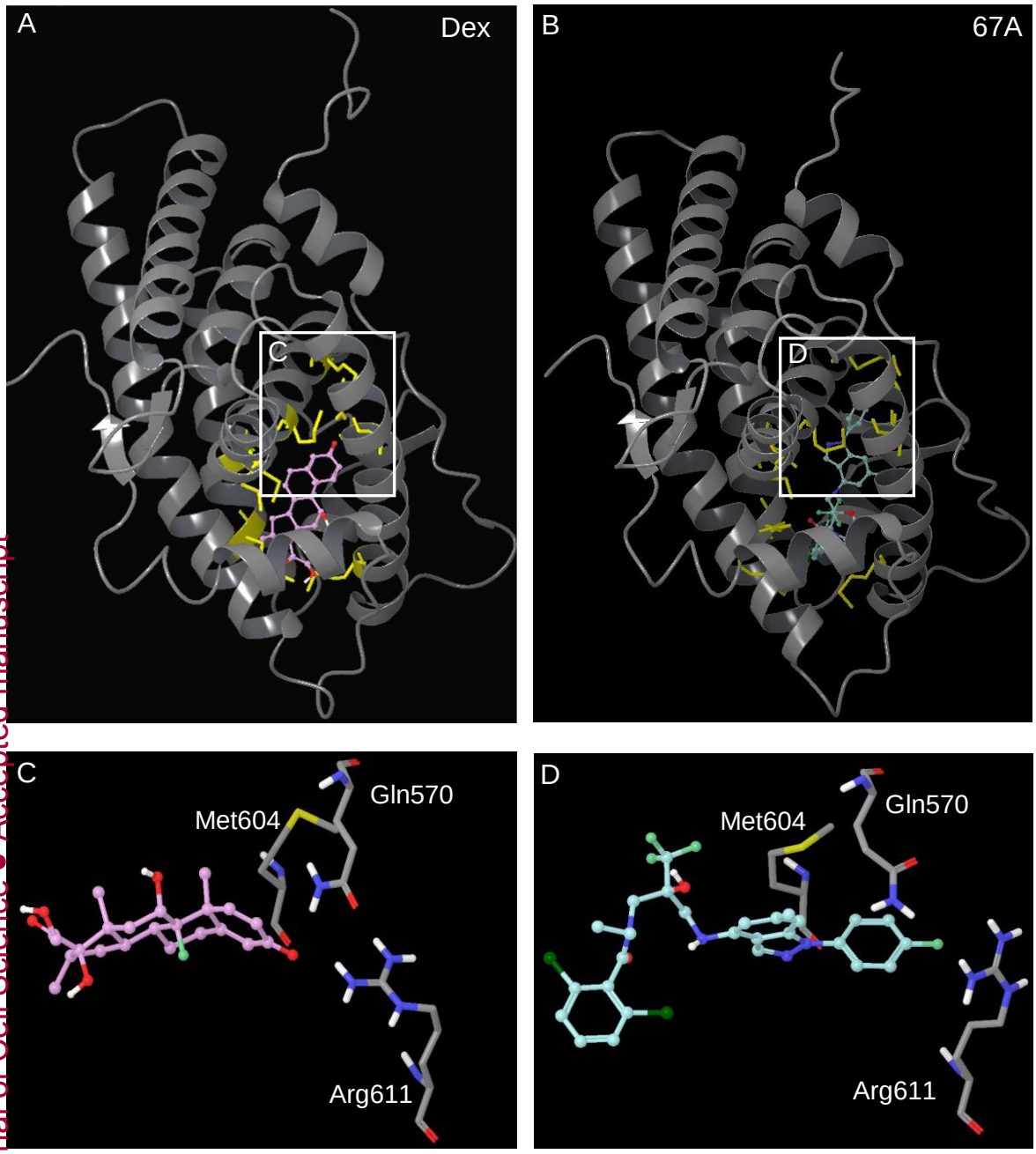

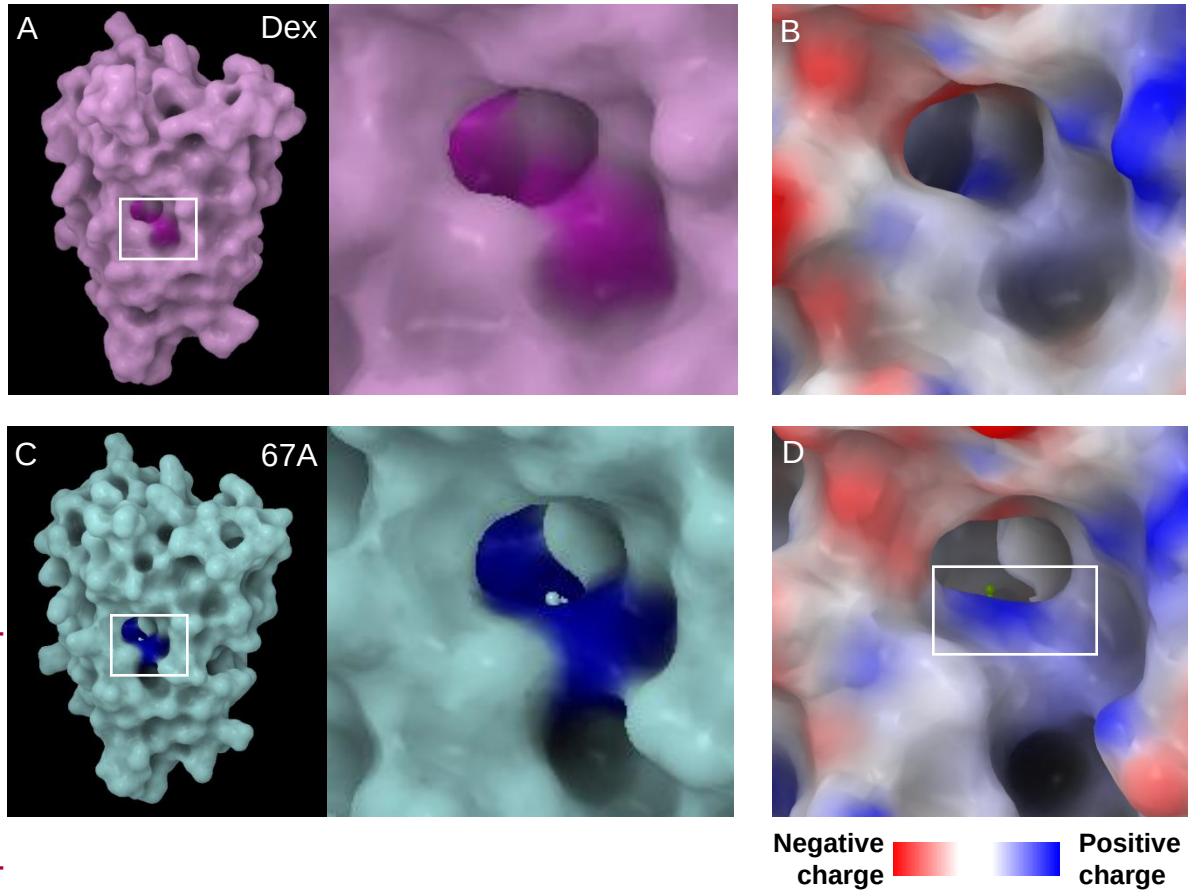

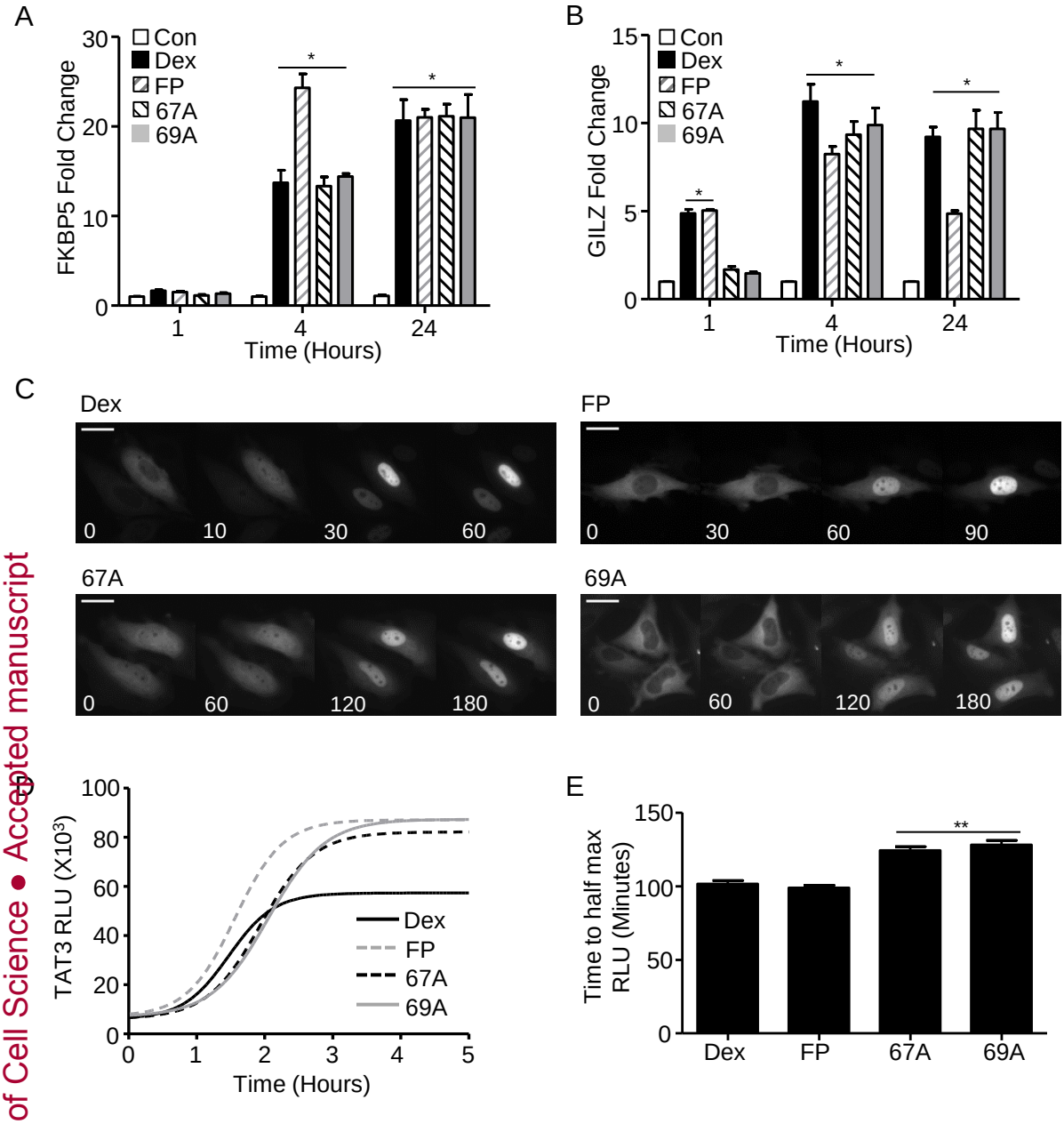

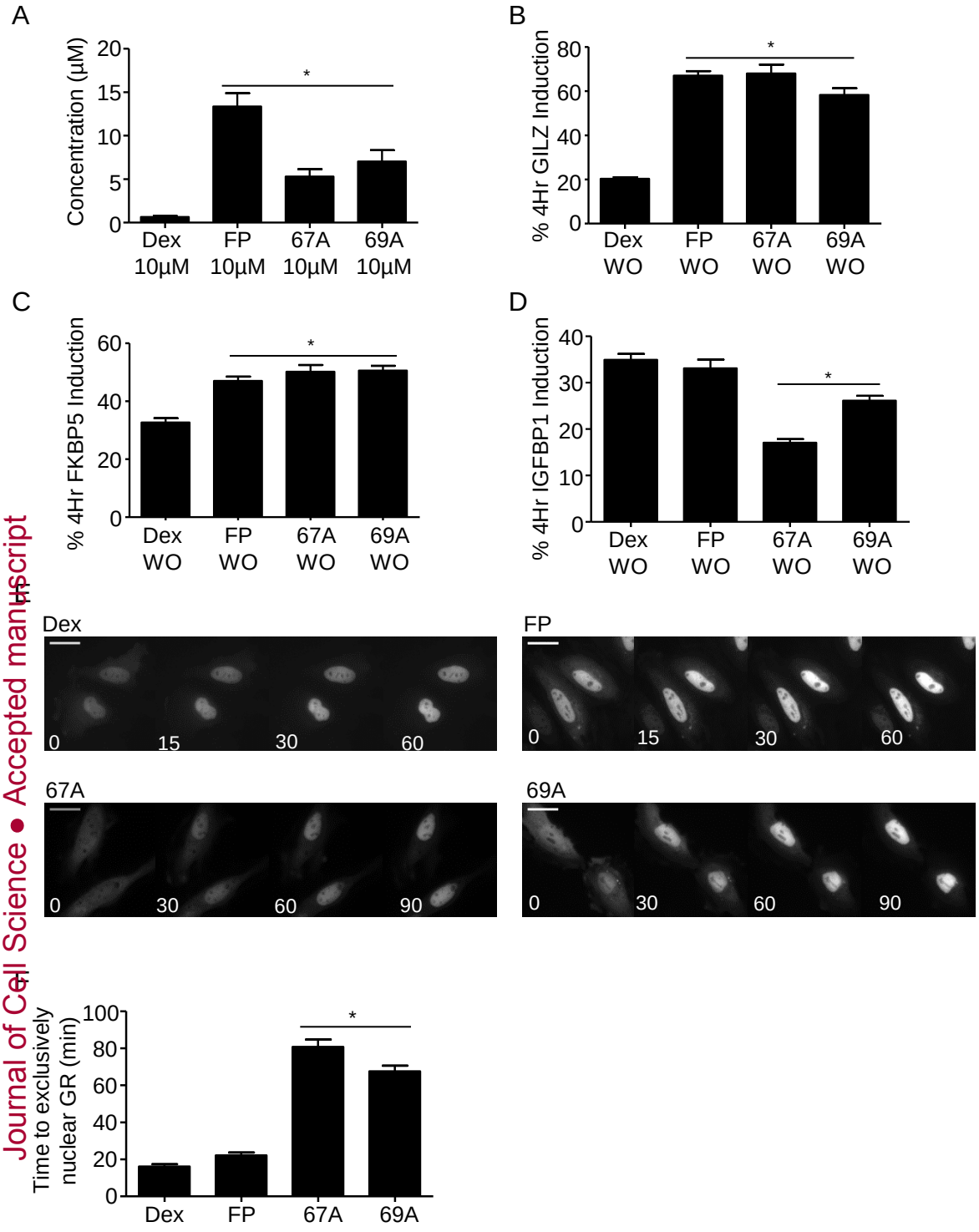

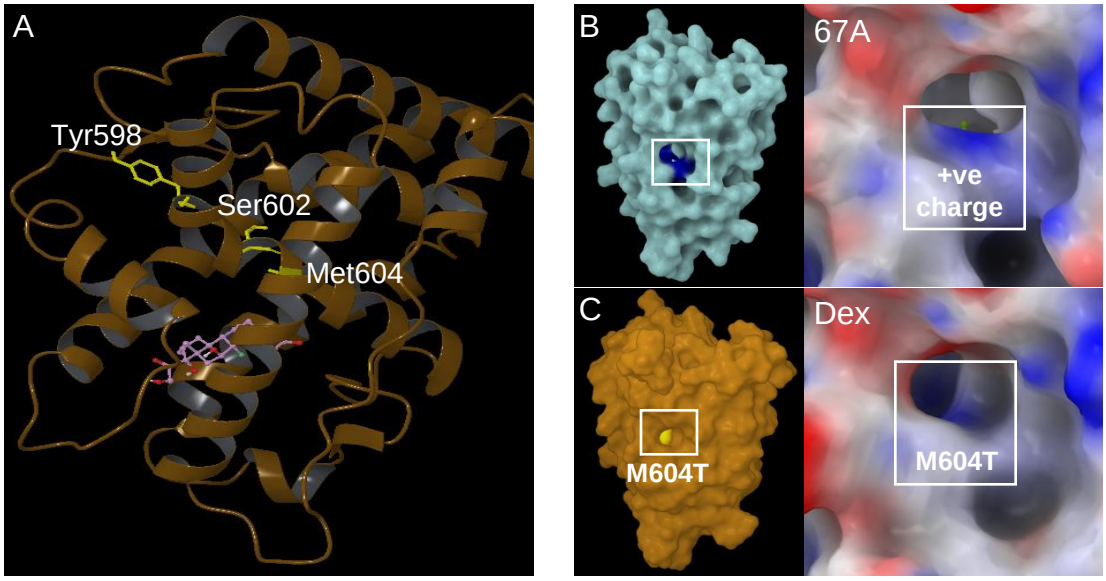

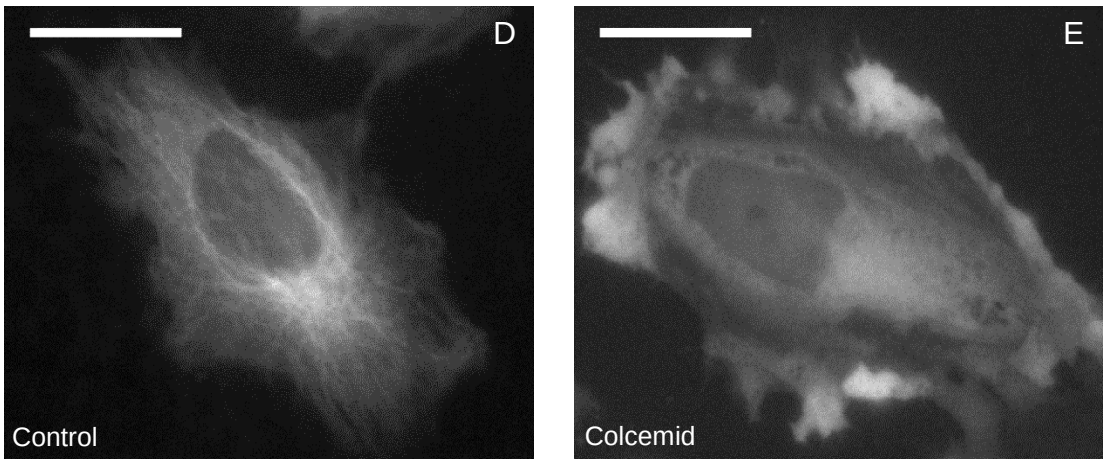

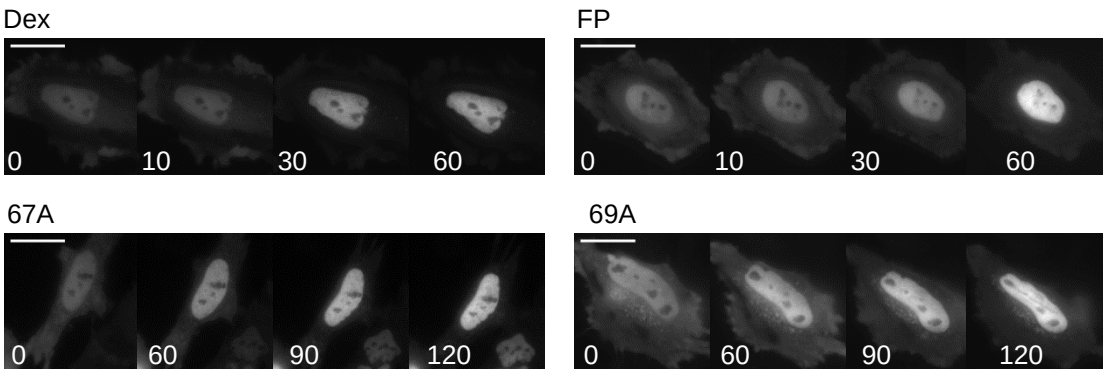

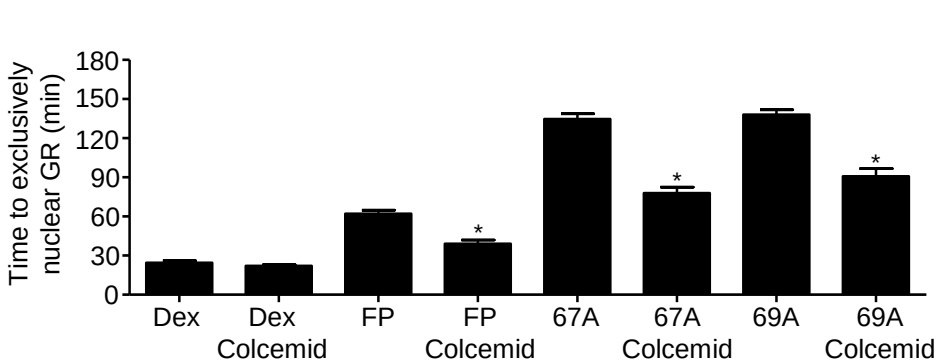

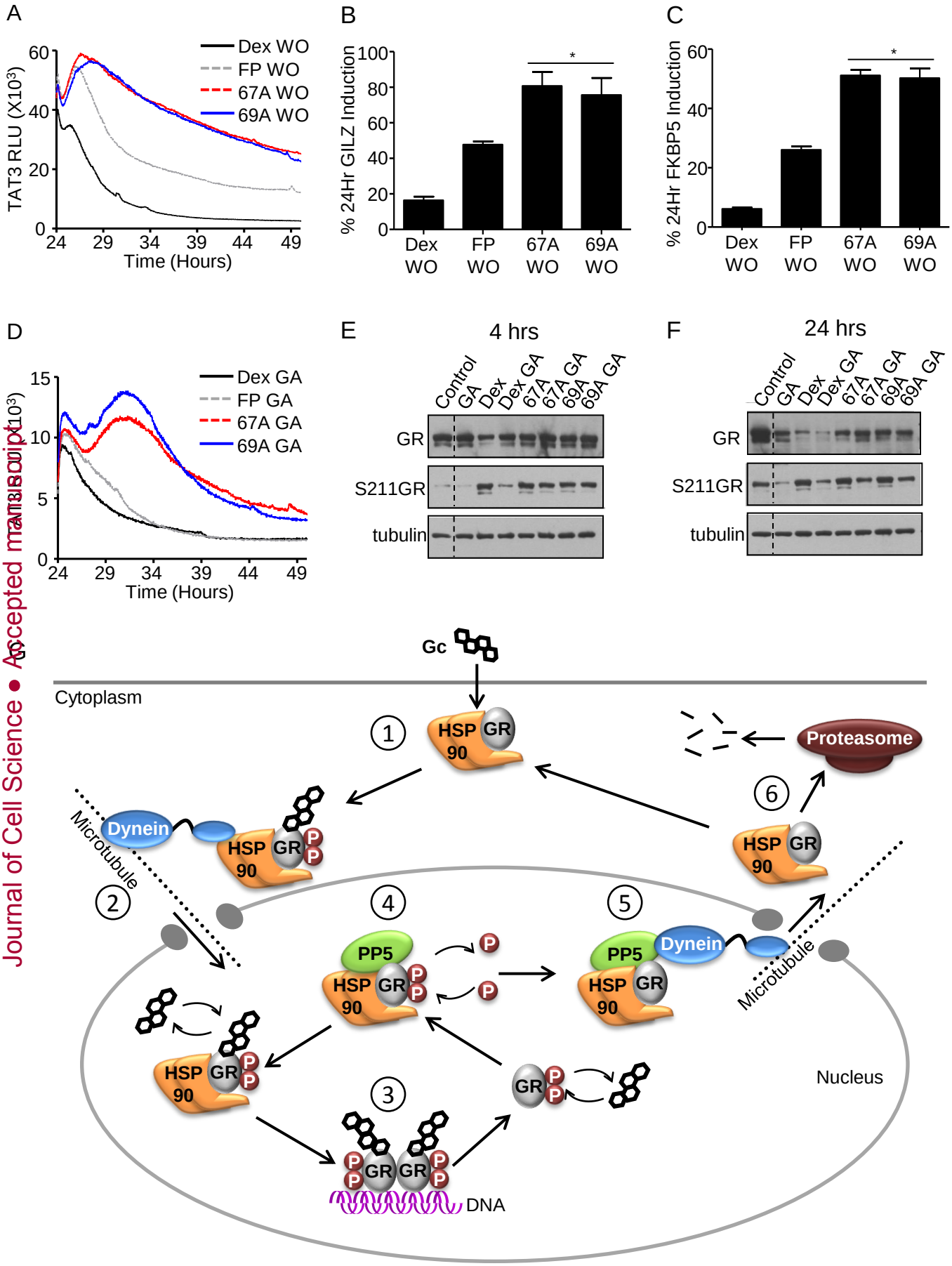

Table 1: Saturating concentration of ligands calculated from EC50.

	Dex	67A	69A
Average EC50	6.26	0.29	0.28
StDev	+/- 3.8	+/- 0.13	+/- 0.06
10x (EC50+StDev)	100nM	3nM	3nM